

Rashba cavity QED: a route towards the superradiant quantum phase transition

Pierre Nataf,¹ Thierry Champel,¹ Gianni Blatter,² and Denis M. Basko¹

¹*Laboratoire de Physique et Modélisation des Milieux Condensés,
Université Grenoble Alpes and CNRS, 25 rue des Martyrs, 38042 Grenoble, France*

²*Institute for Theoretical Physics, ETH Zurich, 8093 Zurich, Switzerland*

(Dated: July 8, 2019)

We develop a theory of cavity quantum electrodynamics for a 2D electron gas in the presence of Rashba spin-orbit coupling and perpendicular static magnetic field, coupled to spatially nonuniform multimode quantum cavity photon fields. We demonstrate that the lowest polaritonic frequency of the full Hamiltonian can vanish for realistic parameters, achieving the Dicke superradiant quantum phase transition. This singular behaviour originates from soft spin-flip transitions possessing a non-vanishing dipole moment at non-zero wave vectors and can be viewed as a magnetostatic instability.

I. INTRODUCTION

The Dicke model, describing an ensemble of identical two-level systems (matter excitations) coupled to a single bosonic (cavity photon) mode, is a prototypical model of cavity quantum electrodynamics (QED) [1]. In the so-called ultrastrong coupling regime [2, 3], when the coupling strength (Rabi frequency) becomes comparable to the energy splitting of the two-level system and that of the photon, the Dicke model was shown to exhibit the so-called superradiant quantum phase transition (SQPT) towards a ground state characterised by a finite static average of the photon field [4, 5]. To the best of our knowledge, this phase transition has never been observed at equilibrium, although ultra-strong coupling regime has been reached in a two-dimensional electron gas (2DEG) in a semiconductor nanostructure placed in a cavity and subject to a perpendicular static magnetic field, so that the matter excitations were represented by the cyclotron resonance [6]. Moreover, a softening of the lowest polaritonic excitation has been recently observed in this system [7].

The Dicke model has an intrinsic flaw: it must be obtained by a reduction of a full microscopic model of some matter system coupled to the electromagnetic field, and typically, the assumptions used to justify this reduction, break down when the model is pushed to the ultrastrong coupling. As a consequence, the SQPT is usually prevented by the so-called “no-go” theorems [8–15]. They express the simple fact that a physical system cannot respond to a static uniform vector potential which can be simply removed by a gauge transformation. On top of the driven-dissipative scenario [16, 17], which has been successfully realized with cold atoms [18], different suggestions have been proposed to circumvent “no-go” theorems at equilibrium. These include systems with magnetic-dipole interactions due to the presence of cavity magnetic fields [19] or its circuit QED analog with an inductive coupling [20, 21] that can be of much larger magnitude [22]. Notably, in the past two decades it has been shown in several works for different physical systems that upon a proper microscopic treatment, the mysterious SQPT assumes a more familiar shape of a ferroelectric [23, 24] or an excitonic insulator [25, 26] instability. In these studies, the crucial role of the Coulomb interaction has been pointed out. In addition, the instability occurred at length scales much shorter than the cavity size,

thereby questioning the very role of the cavity.

In this work, we present a model without Coulomb interaction and still exhibiting a SQPT. Namely, we consider a 2DEG with Rashba spin-orbit coupling, placed inside an optical cavity, and subject to a perpendicular magnetic field B . In the decoupled 2DEG, the Landau levels can cross at certain values of B corresponding to dipole-allowed excitations with zero energy. The presence of such intrinsic soft excitations greatly enhances the effect of the coupling to the transverse electromagnetic field. We develop a theory of Rashba cavity QED for integer filling factors and show that this coupling leads to further softening of the system and appearance of some “superradiant” phases. Crucially, the instability occurs at a finite wave vector of the cavity field; to describe it, all high-energy cavity modes must be included without any truncation in energy. This instability is of magnetostatic nature; the resulting “superradiant” phase is a remote relative of Condon domains of spontaneous magnetization known since long ago for bulk metals in a magnetic field [27]. Moreover, it turns out that this instability can also occur without the cavity: the coupling to the free vacuum field appears sufficient.

II. THE MODEL

It is well known [28] that the effective strength of the light-matter coupling is enhanced if multiple copies of the material system are present. We therefore consider n_{qw} identical quantum wells, each hosting a 2DEG with the single-electron Hamiltonian containing a Rashba coupling term [29],

$$\mathcal{H}_{\text{2DEG}} = \frac{1}{2m^*} (\mathbf{p} + e\mathbf{A}/c)^2 + \alpha [\boldsymbol{\sigma} \times (\mathbf{p} + e\mathbf{A}/c)]_z. \quad (1)$$

Here $\mathbf{p} = -i(\partial_x, \partial_y)$ is the 2D in-plane electron momentum (we set $\hbar = 1$), m^* is the effective mass, $\boldsymbol{\sigma} = (\sigma_x, \sigma_y, \sigma_z)$ is the vector of Pauli matrices, and α is the Rashba spin-orbit coupling constant. Typically, for some existing InSb samples [30], $m^* \simeq 0.02m_0$ (m_0 being the free electron mass), $\alpha \simeq 0.7 \text{ eV} \cdot \text{\AA}$. We assume $e > 0$, the electron charge being $-e$. Finally, the vector potential $\mathbf{A} = \mathbf{A}^{\text{ext}} + \mathbf{A}^{\text{cav}}$ consists of two parts that we discuss separately.

First, $\mathbf{A}^{\text{ext}}(\mathbf{r}) = (-By, 0, 0)$ corresponds to the external magnetic field B , applied perpendicularly to the 2DEG plane

(in the z direction). The resulting single-particle spectrum consists of Landau levels (LLs) with energies

$$\epsilon_{\eta,s} = \omega_c \left(\eta + \frac{s}{2} \sqrt{1 + 8\eta\gamma^2} \right), \quad (2)$$

where $\eta = 0, 1, 2, \dots$ is the LL index, $s = \pm 1$ for $\eta \geq 1$ and $s = 1$ for $\eta = 0$ is what remains of the spin index, $\omega_c = eB/(m^*c)$ is the cyclotron frequency, and $\gamma \equiv \alpha m^* l_B$ with $l_B \equiv (eB/c)^{-1/2}$ being the magnetic length. In Fig. 1, we show the LL energies $\epsilon_{\eta,s}$ for parameters consistent with InSb [30]; the spectrum exhibits crossings that occur between LLs (η_1, s) and $(\eta_2, -s)$ satisfying the conditions [31] $|\eta_1 - \eta_2| > 1$ and

$$\alpha^2 = \frac{\eta_1 + \eta_2 - \sqrt{4\eta_1\eta_2 + 1}}{2(m^*l_B)^2}. \quad (3)$$

Note that levels with the same s never cross. Each Landau level has a degeneracy $L_x L_y / (2\pi l_B^2)$ where $L_x L_y$ is the sample area. We assume to be at zero temperature, at a fixed electron density n_e , and at a magnetic field corresponding to an integer filling factor $\nu \equiv 2\pi l_B^2 n_e$. Indeed, the SQPT is associated with a change in the character of the non-degenerate ground state of a gapped system. Lifting the ground state degeneracy, which occurs at fractional fillings, represents a totally different problem.

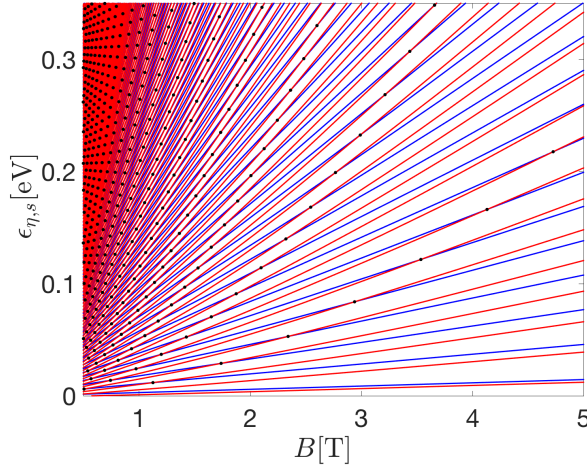


FIG. 1. (color online) LL energies $\epsilon_{\eta,s}$ from Eq. (2) versus B in Tesla. The blue (red) curves correspond to $s = +1$ ($s = -1$). The parameters are $\alpha = 0.7 \text{ eV} \cdot \text{\AA}$ and $m^* = 0.02m_0$. The black points mark the crossings where Eq. (3) is satisfied.

The vector potential $\mathbf{A}^{\text{cav}}(\mathbf{r})$ of the cavity field is defined by the mode expansion, determined by the cavity shape. For simplicity, here we consider a perfect metallic cavity whose dimensions satisfy $L_x \gg L_z \gg L_y$, filled by a material with a dielectric constant ϵ . Then, one can consider only resonator modes with wave vectors $\mathbf{q} = (q_x, 0, q_z)$, where q_x is varying continuously and $q_z = \pi n_z / L_z$, $n_z = 1, 2, 3, \dots$. The corresponding mode frequencies are $\omega_{q_x, n_z}^{\text{cav}} = (c/\sqrt{\epsilon}) \sqrt{q_x^2 + q_z^2}$.

The cavity vector potential then reads [32, 33]

$$\mathbf{A}^{\text{cav}}(\mathbf{r}) = \sum_{q_x, n_z} \sqrt{\frac{4\pi}{L_x L_y L_z \epsilon \omega_{q_x, n_z}}} \mathbf{u}_y \sin \frac{n_z \pi z}{L_z} \times (a_{q_x, n_z} e^{iq_x x} + a_{q_x, n_z}^\dagger e^{-iq_x x}), \quad (4)$$

where a_{q_x, n_z}^\dagger and a_{q_x, n_z} are the photon creation and annihilation operators and \mathbf{u}_y is the unit vector in the y direction. We assume the whole 2DEG sample with n_{qw} quantum wells to be much thinner than L_z and placed in the middle of the cavity. Then, what enters Eq. (1), is $\mathbf{A}_{\text{cav}}(z = L_z/2)$ and the modes with even n_z are decoupled.

III. POLARITON MODES AND INSTABILITY

The ‘‘superradiant’’ instability is signalled by the vanishing of the lowest polariton frequency. To find the polariton modes – the excitations of the coupled 2DEG-cavity system – one can proceed in several ways. For example, similarly to that adopted in Ref. [33] for the same problem without spin-orbit coupling, one writes the 2DEG many-body Hamiltonian in terms of creation and annihilation operators for inter-LL excitations, which are approximately bosonic; then the full Hamiltonian of the 2DEG and the cavity becomes bilinear in the bosonic operators and thus can be diagonalized by the appropriate Bogoliubov transformation. Alternatively, one can write the (zero-temperature or Matsubara) action for coupled electron and photon fields, integrate out the electrons, and expand the resulting bosonic action to the second order in the photon vector potential. Both (rather standard) calculations are given in the respective appendices A and B, and their equivalence is checked explicitly.

As a result, the polariton frequencies are given by the solutions of the equation

$$\frac{c}{2\pi} \sqrt{c^2 q_x^2 - \epsilon \omega^2} \coth \frac{L_z \sqrt{q_x^2 - \epsilon \omega^2 / c^2}}{2} = -Q_{yy}(q_x, \omega), \quad (5)$$

where $Q_{yy}(q_x, \omega)$ is the susceptibility determining the linear response $\hat{j}_y = Q_{yy}(\delta A_y / c) e^{iq_x x - i\omega t}$ of the 2D electron current density \hat{j}_y to a perturbing vector potential $\delta \mathbf{A}$ on top of \mathbf{A}^{ext} included in the unperturbed system, $\mathbf{A} = \mathbf{A}^{\text{ext}} + \delta \mathbf{A} e^{iq_x x - i\omega t}$. The susceptibility consists of two contributions, the diamagnetic one and the sum over all inter-LL transitions in all quantum wells,

$$Q_{yy}(q_x, \omega) = \frac{n_{\text{qw}} n_e e^2}{m^*} \left[1 - \frac{\omega_c}{\nu} \sum_{\ell \leq \nu < \ell'} \frac{\omega_{\ell' \ell}^{\text{LL}} [g_{q_x}^{\ell' \ell}]^2}{(\omega_{\ell' \ell}^{\text{LL}})^2 - \omega^2} \right]. \quad (6)$$

Here the LL indices $(\eta, s) \equiv \ell$ are combined into a single label, ordered according to the LL energies ϵ_ℓ , Eq. (2), so that LLs with $\ell \leq \nu$ are filled, and those with $\ell > \nu$ are empty. The transition energy $\omega_{\ell' \ell}^{\text{LL}} \equiv \epsilon_{\ell'} - \epsilon_\ell$, and the reduced coupling

constants $g_{q_x}^{\ell'\ell}$ (dipole matrix elements) are defined as

$$g_{q_x}^{\ell'\ell} = -\sqrt{2}\gamma \left(\sin\theta_{\ell'} \cos\theta_{\ell} \Theta_{\eta'-1}^{\eta} - \cos\theta_{\ell'} \sin\theta_{\ell} \Theta_{\eta'-1}^{\eta-1} \right) + \sin\theta_{\ell'} \sin\theta_{\ell} \left(\sqrt{\eta-1} \Theta_{\eta'-1}^{\eta-2} - \sqrt{\eta} \Theta_{\eta'-1}^{\eta} \right) + \cos\theta_{\ell'} \cos\theta_{\ell} \left(\sqrt{\eta} \Theta_{\eta'-1}^{\eta-1} - \sqrt{\eta+1} \Theta_{\eta'-1}^{\eta+1} \right), \quad (7)$$

where $\tan\theta_l = [-1 + s\sqrt{1 + 8\eta\gamma^2}]/(\sqrt{8\eta\gamma})$, and the overlap function $\Theta_{n_2}^{n_1}$ containing the q_x dependence is given by

$$\Theta_{n_2}^{n_1} = \sqrt{\frac{m!}{M!}} e^{-\frac{\xi}{2}} \xi^{\frac{M-m}{2}} L_m^{M-m}(\xi) S^{n_2-n_1}, \quad (8)$$

with $L_m^{M-m}(\xi)$ the generalized Laguerre polynomial of $\xi \equiv l_B^2 q_x^2/2$, $S = \text{sign}[q_x(n_2 - n_1)]$, $m = \min\{n_1, n_2\}$, and $M = \max\{n_1, n_2\}$. Since at $q_x = 0$ we have $\Theta_{n_2}^{n_1} = \delta_{n_1, n_2}$, the reduced coupling constants $g_{q_x=0}^{\ell'\ell}$ are non-zero only between consecutive LLS, $\eta' = \eta \pm 1$, with no restriction on s . In contrast, at finite q_x , this selection rule is relaxed.

Equations (5)–(8) represent the main analytical result of this paper. Note that in Eq. (5) all information about the cavity is on the left-hand side, while all information about the 2DEG is on the right. At $\omega = 0$ (i.e., at the sought superradiant transition) the left-hand side is proportional to c^2 which is much larger than any velocity scale occurring in a typical solid. Moreover, when $\omega = 0$, the second term of the right-hand side of Eq. (6) is nothing but the total sum of the oscillator strengths $|g_{q_x}^{\ell'\ell}|^2/\omega_{\ell'\ell}^{\text{LL}}$, which is the fundamental quantum optics quantity that determines the occurrence of the SQPT in multilevel systems coupled to cavity fields [11]. It diverges at the level crossing, balancing the large c^2 factor in the left-hand side and allowing the existence of a solution to Eq. (5).

The key reason is that for the spin-flip transitions at $q_x \neq 0$, the dipoles $g_{q_x}^{\ell',\ell}$ can be non-zero even at a crossing between $\epsilon_{\ell'}$ and ϵ_{ℓ} , opening the possibility of a diverging oscillator strength. In Fig. 2, we present an example of such crossing. This is in sharp contrast with what happens at $q_x = 0$, where gauge invariance demands the vanishing of the dipole between eigenstates of equal energy (i.e., at the crossings of energy levels), which is at the heart of many no-go theorems regarding the Dicke SQPT for spatially uniform cavity fields [8–11, 13, 15].

Indeed, for a generic single-electron Hamiltonian \mathcal{H} , after the minimal coupling replacement of the electron momentum $\mathbf{p} \rightarrow \mathbf{p} + (e/c)\mathbf{A}_{\text{cav}}$, where \mathbf{A}_{cav} is the uniform cavity field, the matrix element of the linear light-matter coupling term between two arbitrary eigenstates $|1\rangle, |2\rangle$ of \mathcal{H} , is proportional to that of the electron velocity $\mathbf{v} = \partial\mathcal{H}/\partial\mathbf{p} = i[\mathcal{H}, \mathbf{r}]$, so that $\mathbf{v}_{12} = \langle 1|[\mathcal{H}, \mathbf{r}]|2\rangle = (\epsilon_1 - \epsilon_2)\langle 1|\mathbf{r}|2\rangle$. Then, at the crossing $\epsilon_1 - \epsilon_2$ vanishes, and both the velocity matrix element \mathbf{v}_{12} and the oscillator strength $\propto |\mathbf{v}_{12}|^2/(\epsilon_1 - \epsilon_2)$ vanish. Crucially, this argument does not apply to spatially non-uniform fields.

From a different perspective, gauge invariance imposes a constraint on $Q_{yy}(q_x, \omega)$: a physical quantity (current) cannot respond to a static spatially homogeneous vector potential, thus $Q_{yy}(0, 0) = 0$. This prohibits the instability at $q_x = 0$; models or approximations violating this constraint

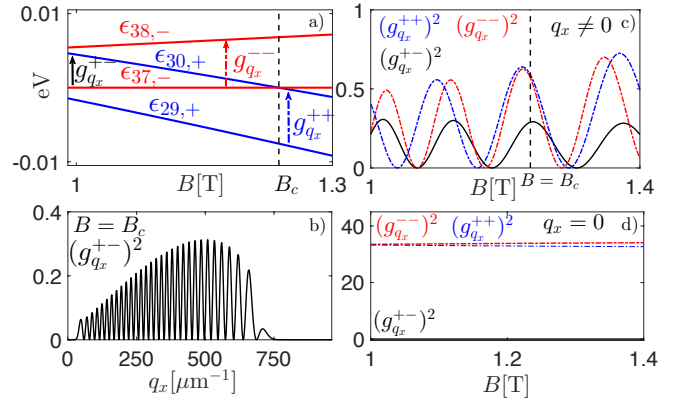


FIG. 2. (color online) a) LL energies $\epsilon_{29,+}$, $\epsilon_{30,+}$, $\epsilon_{37,-}$, $\epsilon_{38,-}$ in eV [see Eq. (2)] as a function of B (in Tesla) for the same parameters as in Fig. 1. The gap closes between the states $|37, -\rangle$ and $|30, +\rangle$ at $B_c \simeq 1.23721$ T. In b), we plot the square of the spin-flip dipole $(g_{q_x}^{+-})^2 \equiv (g_{q_x}^{30+,37-})^2$ [see Eq. (7)] as a function of q_x at $B = B_c$. At $q_x = 0$, it vanishes as a consequence of gauge invariance. When q_x increases, it oscillates and takes non-zero values, opening the possibility of a diverging oscillator strength proportional to $(g_{q_x}^{+-})^2/(\epsilon_{30,+} - \epsilon_{37,-})^2$. Finally, we plot $(g_{q_x}^{+-})^2$, $(g_{q_x}^{++})^2$ and $(g_{q_x}^{--})^2$ as a function of B for $q_x = 4 \times 10^8 \text{ m}^{-1}$ in c) and $q_x = 0$ in d).

can give wrong results. $Q_{yy}(0, 0) = 0$ implies a cancellation between the two terms in Eq. (6). This cancellation is usually ensured by sum rules such as the famous Thomas-Reiche-Kuhn strength of localized atomic systems [8–13, 15]. Here, we have checked it numerically.

In Fig. 3(a), we plot the two sides of Eq. (5) at $\omega = 0$ as functions of the cavity field wave-vector q_x and show six values of $q_x > 0$ (shown in magenta dashed lines) when $\omega = 0$ is a solution. In Fig. 3(b), we display the lowest polariton frequency $\omega_{q_x}^{\text{pol}}$ which indeed vanishes at the indicated values of q_x . Between two values of q_x where Eq. (5) is satisfied at $\omega = 0$, the left-hand side of Eq. (5) is smaller than the right-hand side and the system is in the “superradiant” phase. In the inset of Fig. 3(a), we plot the two sides of Eq. (5) at $\omega = 0$ as a function of B for a given value of q_x , for $n_{\text{qw}} = 1$ and $n_{\text{qw}} = 10^3$. Essentially, we exploit a divergence appearing around level crossings to make Eq. (5) have a solution, and then use large n_{qw} to have an extended regime for the superradiant phase.

Fig. 4 shows the phase diagram in the plane (α, q_x) , for fixed magnetic field B and filling ν . The “superradiant” phase appears for nonzero q_x and for values of α very close to those given by Eq. (3) for some integers $\eta_1 \neq \eta_2$ satisfying $\eta_1 + \eta_2 = \nu$, and depicted in dashed red lines in Fig. 4. The characteristic width $\Delta\alpha$ of the “superradiant” regions on the phase diagram can be estimated as (see Appendix C)

$$\Delta\alpha \sim \frac{1}{\nu^2} \frac{n_{\text{qw}} n_e e^2}{(m^* c)^2}, \quad (9)$$

and the typical scale of q_x is given by the inverse cyclotron radius, $(\sqrt{\nu} l_B)^{-1}$. The “superradiant” regions are very narrow; this happens because the mechanism for the instability can be

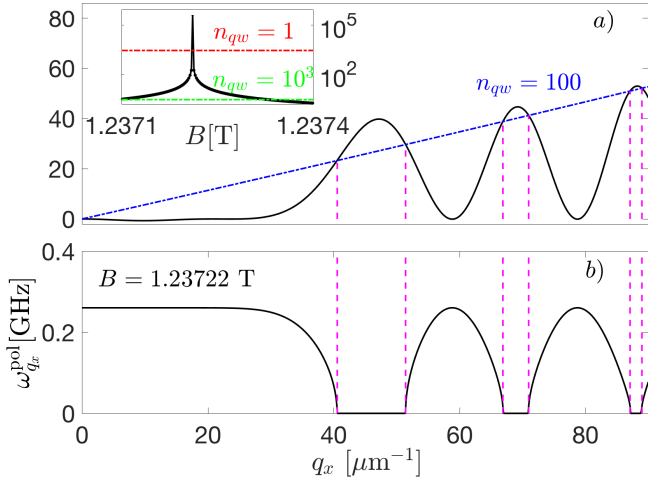


FIG. 3. (color online) a) The two sides of Eq. (5) at $\omega = 0$ divided by $(n_{\text{qw}} n_e e^2 / m^*)$ (the solid black curve for the right-hand side and the dash-dotted blue one for the left-hand side, plotted versus q_x (in μm^{-1}) for $B = 1.23722$ T [which exceeds B_c , cf Fig. 2 (a)] for $\alpha = 0.7$ eV \cdot \AA , $m^* = 0.02 m_0$ and $\nu = 67$, $L_z = 20$ μm , $\varepsilon = 10$, $n_{\text{qw}} = 100$. The crossings of the two quantities give solutions of Eq. (5) for q_x at $\omega = 0$ (vanishing polariton frequency). In the inset, same quantities plotted as a function of B for $q_x = 4.8 \times 10^7$ m^{-1} , where the red (resp. green) correspond to $n_{\text{qw}} = 1$ (resp. $n_{\text{qw}} = 1000$). At $B = 1.23722$ T, it happens at values of q_x shown by the vertical dashed lines for $n_{\text{qw}} = 100$. The lowest polariton mode $\omega_{q_x}^{\text{pol}}$, plotted in b), vanishes at these values.

traced to the magnetostatic interaction, as we discuss below. Typically, one arrives at the Dicke model assuming the light-matter coupling via the cavity electric field. However, this electric field, $\propto \partial \mathbf{A}_{\text{cav}} / \partial t$, vanishes at $\omega = 0$. The remaining magnetic interaction is intrinsically weak. These simple physical arguments are not obvious from the equations.

From Eq. (9) and Fig. 4 we see that small filling factors are favoring the “superradiant” phase. This is in stark contrast to the condition of $\nu \gg 1$ formulated in Ref. [33] to achieve the ultrastrong coupling regime. Again, the reason for this difference is that the SQPT obtained here is determined by the magnetic coupling and not the electric one.

IV. SQPT AS A MAGNETOSTATIC INSTABILITY

Consider the 2DEG in free space (no cavity). When placed in a static homogeneous magnetic field $\mathbf{B}^{\text{ext}}(\mathbf{r}) = B \mathbf{u}_z$, it develops a static equilibrium magnetization $\mathbf{M}^{\text{eq}}(\mathbf{r}) = M^{\text{eq}} \mathbf{u}_z \delta(z - L_z/2)$. Let us see at what conditions the system can spontaneously develop an additional inhomogeneous magnetization $\delta \mathbf{M}(\mathbf{r})$ which would produce an inhomogeneous magnetic field. Equivalently, we study the stability of the described equilibrium configuration with respect to a small perturbation, $\mathbf{B} = \mathbf{B}^{\text{ext}} + \delta \mathbf{B}(\mathbf{r})$.

We look for static magnetic field configurations $\delta \mathbf{B}(\mathbf{r})$

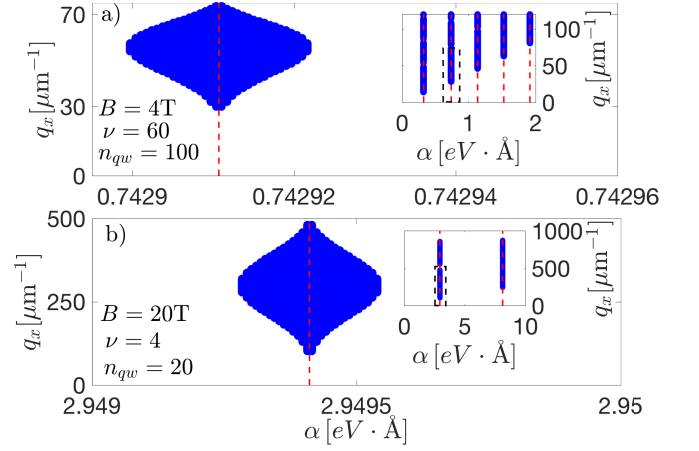


FIG. 4. (color online) Phase diagrams of the “superradiant” phase (in blue) in the parameter plane (α, q_x) for different B , ν and n_{qw} . The inset display the phase diagrams for a larger range of parameters. Values of α for which there is an energy crossing [cf Eqs. (2) and (3)] are depicted in dashed red lines. The “superradiant” phases occur around these crossings. a) $B = 4$ T, $\nu = 60$ and $n_{\text{qw}} = 100$; b) $B = 20$ T, $\nu = 4$ and $n_{\text{qw}} = 20$.

which minimize the classical free energy functional

$$F[\delta \mathbf{B}] = \int \left[\frac{(\mathbf{B}^{\text{ext}} + \delta \mathbf{B})^2}{8\pi} - \mathbf{M}^{\text{ext}} \cdot \delta \mathbf{B} \right] d^3 \mathbf{r} + \int \left[-\mathbf{M}^{\text{eq}} \cdot \delta \mathbf{B} - \frac{1}{2} \chi_{kl} \delta B_k \delta B_l + \dots \right] d^3 \mathbf{r}, \quad (10)$$

under the constraint $\nabla \cdot \delta \mathbf{B} = 0$. The first line contains the energy density of the free field as well as the contribution due to \mathbf{M}^{ext} , the magnetization of the currents which produce \mathbf{B}^{ext} . The second line is the free energy of the 2DEG.

Its quadratic part is determined by the static magnetic susceptibility $\chi_{ij}(\mathbf{r}, \mathbf{r}')$, which gives the response of the magnetization $\delta \mathbf{M}$ to a magnetic field perturbation $\delta \mathbf{B}$ on top of \mathbf{B}^{ext} . Since $\mathbf{B} = \nabla \times \mathbf{A}$, and the static current density \mathbf{j} can be written in terms of the magnetization \mathbf{M} as $\mathbf{j} = c \nabla \times \mathbf{M}$, the susceptibility χ is related to the current response $Q(\omega = 0)$ found earlier on,

$$\chi_{zz}(\mathbf{r}, \mathbf{r}') = - \int \frac{dq_x}{2\pi} e^{iq_x(x-x')} \frac{Q_{yy}(q_x, \omega = 0)}{c^2 q_x^2} \times \delta(y-y') \delta(z-L_z/2) \delta(z'-L_z/2). \quad (11)$$

Here $\delta(y-y')$ appears because our starting model was restricted to a y -independent $\mathbf{A}_{\text{cav}}(\mathbf{r})$, see Eq. (4).

Varying $F + \int \lambda(\mathbf{r}) \nabla \cdot \mathbf{B} d^3 \mathbf{r}$ with the Lagrange multiplier $\lambda(\mathbf{r})$, we arrive at the equations

$$\mathbf{B}^{\text{ext}} + \delta \mathbf{B}(\mathbf{r}) = 4\pi \mathbf{M}(\mathbf{r}) + \nabla \int \frac{d^3 \mathbf{r}'}{|\mathbf{r} - \mathbf{r}'|} \nabla' \cdot \mathbf{M}(\mathbf{r}'), \quad (12a)$$

$$M_k(\mathbf{r}) = M_k^{\text{ext}}(\mathbf{r}) + M_k^{\text{eq}}(\mathbf{r}) + \int \chi_{kl}(\mathbf{r}, \mathbf{r}') \delta B_l(\mathbf{r}') d^3 \mathbf{r}'. \quad (12b)$$

In Eq. (12a), the terms containing \mathbf{B}^{ext} and \mathbf{M}^{ext} cancel out by construction; the terms with \mathbf{M}^{eq} drop out because a magnetization $\propto \mathbf{u}_z \delta(z - L_z/2)$ does not produce any magnetic field except near the sample edges; thus, Eq. (12a) becomes a linear homogeneous equation for $\delta\mathbf{B}(\mathbf{r})$. The existence of a non-trivial solution corresponds to a direction along which the quadratic form in Eq. (10) is flat.

Let us try the modulation

$$\delta\mathbf{M}(\mathbf{r}) = M_{q_x} \mathbf{u}_z \delta(z - L_z/2) e^{iq_x x}, \quad (13)$$

with some $q_x > 0$. The solution of Eq. (12a) for $\delta\mathbf{B}$,

$$\begin{aligned} \delta B_x(\mathbf{r}) &= -2i\pi q_x M_{q_x} e^{-q_x |z - L_z/2| - iq_x x} \text{sign}(z - L_z/2), \\ \delta B_z(\mathbf{r}) &= 2\pi q_x M_{q_x} e^{-q_x |z - L_z/2| - iq_x x}, \end{aligned} \quad (14)$$

when substituted in Eq. (12b), gives the magnetostatic instability condition

$$-2\pi q_x \frac{Q_{yy}(q_x, \omega = 0)}{c^2 q_x^2} = 1. \quad (15)$$

This condition is identical to Eq. (5) at $\omega = 0$ in the limit $L_z \rightarrow \infty$, that is, in the absence of the cavity.

The obtained modulational instability of the magnetization is long known for bulk paramagnetic materials in an external magnetic field, where it gives rise to the so-called Condon domains of different magnetization [27]. Indeed, such a domain structure has the characteristics of the ‘‘superradiant’’ phase: the magnetic field produced by the domains corresponds to a non-zero expectation value of the photon field $\langle a_{q_x, n_z} \rangle$. On the other hand, while the superradiant phase in the Dicke model spontaneously breaks the Z_2 symmetry associated with the sign of the spontaneously generated uniform cavity field [5] (variations of the model with higher symmetries have also been considered [4, 34, 35]), the domain structure obtained here spontaneously breaks at least the continuous translation symmetry. In particular, for a sinusoidal modulation the Z_2 sign flip is equivalent to translating the pattern by half a period. To make precise statements about the broken symmetries, one would need a detailed quantitative study of the ‘‘superradiant’’ phase and of the resulting magnetization profile; such a study is beyond the scope of the present paper.

V. CONCLUSIONS AND OUTLOOK

We have proved that the SQPT can be reached in a cavity QED system with Rashba spin-orbit coupling and non-uniform cavity resonator fields. Within our model, the appearance of the SQPT is a consequence of the singularity of the spin-flip transitions, for which the spin-flip dipole at the field wave-vector $q_x \neq 0$ can be non-zero even if the transition energy vanishes. Consequently, the SQPT must occur close to LLs energy crossings (see Figs. 3 and 4), and requires relatively fine tuning of the magnetic field and electron density, as well as large n_{qw} . We have shown that the SQPT can be viewed as a magnetostatic instability of the 2DEG, the static cavity field corresponding to the magnetic field induced

by a spatially modulated 2DEG magnetization. Moreover, the presence of the cavity is not necessary: it can also happen via the coupling to the free vacuum field.

The microscopic model we studied in this paper has the minimal number of ingredients necessary to produce SQPT. To make a connection with state of the art experiments [6, 7], several other ingredients must be introduced. Zeeman coupling of the 2DEG to the magnetic field is likely to enhance the effect since the spin contribution to the magnetic susceptibility is usually paramagnetic. Coulomb interaction is also likely to further soften the excitations due to the excitonic effect. A very important ingredient is the disorder which lifts the LL degeneracy and broadens the cyclotron resonance. Coherent state based methods have been quite successful in describing the local density of states in a 2DEG with smooth disorder in a strong magnetic field [31, 36]; the effect of smooth disorder on the inter-LL transitions remains an open problem. Effects of strain, as well as mixing between bands with different spins (through, for instance, the multiband Luttinger 6×6 $\mathbf{k} \cdot \mathbf{p}$ model [37]), which both importantly impact the amplitude and the nature of the Rashba coupling [38–40], could also be studied. Finally, adapting our calculations to some other cavities, like the Split Ring Resonator (SSR) and Complementary SRR [41], where an additional geometric factor can enhance the light matter interaction, could also be useful. Finally, in this paper, we focused on the instability, leaving aside the study of the ‘‘superradiant’’ phase itself, a topic that deserves future investigation as well. Moreover, the new physical ingredients listed above, will also be important in determining the properties of the ‘‘superradiant’’ phase.

ACKNOWLEDGMENTS

We acknowledge fruitful discussions with Tobias Wolf, Matteo Biondi, Jérôme Faist, Giacomo Scalari, Janine Keller, Maksym Myronov, Rai Moriya, Takaaki Koga, Roland Winkler, Cristiano Ciuti and David Hagenmüller.

Appendix A: Bogoliubov transformation approach

The single-electron eigenstates of Hamiltonian (1) with the external vector potential $\mathbf{A}_{\text{ext}} = (-By, 0, 0)$ are labeled by $\ell \equiv (\eta, s)$ and p_x , the momentum in the x direction, taken as an integer multiple of $2\pi/L_x$, with L_x being the sample length the x direction. It is convenient to order ℓ according to the energies ϵ_ℓ , given by Eq. (2). The spinor wave functions of the eigenstates are

$$\psi_{\eta, s, p_x}(x, y) = \frac{e^{ip_x x}}{\sqrt{L_x}} \begin{pmatrix} \sin \theta_{\eta s} \phi_{\eta-1}(y - p_x l_B^2) \\ i \cos \theta_{\eta s} \phi_\eta(y - p_x l_B^2) \end{pmatrix}, \quad (A1)$$

with $\tan \theta_{\eta s} = -u_\eta + s\sqrt{1 + u_\eta^2}$, $u_\eta = 1/(\sqrt{8}\eta\gamma)$ and the harmonic oscillator wave functions

$$\phi_\eta(y) = \frac{e^{-y^2/(2l_B^2)}}{\sqrt{2^n \eta! l_B \sqrt{\pi}}} H_\eta(y/l_B), \quad (A2)$$

where H_η is the Hermite polynomial of degree η . The many-body ground state of the 2DEG without coupling to the cavity is

$$|F\rangle = \prod_{j=1}^{n_{\text{qw}}} \prod_{\ell \leq \nu} \prod_{p_x} c_{j,\ell,p_x}^\dagger |0\rangle, \quad (\text{A3})$$

where $|0\rangle$ is the vacuum, c_{j,ℓ,p_x}^\dagger is the fermionic creation operator for an electron on the level ℓ with momentum p_x in the j th quantum well. The product over p_x goes over all $L_x L_y / (2\pi l_B^2)$ allowed values. Cavity photons induce collective electronic excitations which can be described by the approximately bosonic bright modes creation operator, defined for ℓ, ℓ' such that $\epsilon_\ell \leq \epsilon_\nu < \epsilon_{\ell'}$:

$$b_{q_x, \ell' \ell}^\dagger = \sqrt{\frac{2\pi l_B^2}{n_{\text{qw}} L_x L_y}} \sum_{j,p_x} c_{j,\ell',p_x+q_x}^\dagger c_{j,\ell,p_x}, \quad (\text{A4})$$

where the sum runs over the $n_{\text{qw}} L_x L_y / (2\pi l_B^2)$ individual excitation between filled and empty LLs ℓ and ℓ' , respectively.

The full light-matter Hamiltonian H contains four terms:

$$H = H_{\text{cav}} + H_{\text{dia}} + H_{2\text{DEG}} + H_{\text{int}}. \quad (\text{A5})$$

The free cavity photon part is

$$H_{\text{cav}} = \sum_{q_x, n_z} \omega_{q_x, n_z}^{\text{cav}} a_{q_x, n_z}^\dagger a_{q_x, n_z}. \quad (\text{A6})$$

The diamagnetic part of the light-matter interaction arises from the $\mathbf{A}_{\text{cav}}^2$ term in the single-particle Hamiltonian (1):

$$H_{\text{dia}} = \sum_{q_x, n_z, n'_z} D_{q_x}^{n_z, n'_z} a_{q_x, n_z} \left(a_{-q_x, n'_z} + a_{q_x, n'_z}^\dagger \right) + \text{h. c.}, \quad (\text{A7a})$$

$$D_{q_x}^{n_z, n'_z} = \frac{2\pi n_{\text{qw}} n_e e^2}{\epsilon L_z m^* \sqrt{\omega_{q_x, n_z}^{\text{cav}} \omega_{q_x, n'_z}^{\text{cav}}}} \sin \frac{n_z \pi}{2} \sin \frac{n'_z \pi}{2}. \quad (\text{A7b})$$

$H_{2\text{DEG}}$ stands for the electronic part of the Hamiltonian, which can be written using the operators in (A4), as:

$$H_{2\text{DEG}} = \sum_{q_x} \sum_{\ell \leq \nu < \ell'} \omega_{\ell' \ell}^{\text{LL}} b_{q_x, \ell' \ell}^\dagger b_{q_x, \ell' \ell}. \quad (\text{A8})$$

The corresponding energy differences $\omega_{\ell' \ell}^{\text{LL}} = \epsilon_{\ell'} - \epsilon_\ell$ are associated to each transition across the Fermi level. Finally, the linear in \mathbf{A}_{cav} term produces

$$H_{\text{int}} = \sum_{q_x, n_z} \sum_{\ell \leq \nu < \ell'} i \Omega_{q_x, n_z}^{\ell' \ell} \left(a_{q_x, n_z} + a_{-q_x, n_z}^\dagger \right) b_{q_x, \ell' \ell}^\dagger + \text{h.c.}, \quad (\text{A9})$$

where the ℓ, ℓ' sum is again over $\epsilon_\ell \leq \mu \leq \epsilon_{\ell'}$, and the Rabi frequencies for each transition are determined by matrix elements of $e^{iq_x x} (-i\partial_y / m^* - \alpha \sigma_x)$ between different Landau level states:

$$\Omega_{q_x, n_z}^{\ell' \ell} = \sqrt{n_{\text{qw}} \frac{(e^2/c)}{\epsilon \omega_{q_x, n_z}^{\text{cav}} L_z / c} \frac{\sin(n_z \pi / 2)}{m^* l_B^2}} g_{q_x}^{\ell' \ell}, \quad (\text{A10})$$

and the reduced coupling constants (dipole matrix elements) $g_{q_x}^{\ell' \ell}$ are defined in Eq. (7).

In the following, we prove that the eigenfrequencies of the quadratic light-matter Hamiltonian H , shown in (A5) can vanish for some wave vectors q_x . Looking for the bosonic magnetopolariton modes in the form

$$p_{q_x} = W_{q_x} a_{q_x} + Y_{q_x} a_{-q_x}^\dagger + \sum_{\ell \leq \nu < \ell'} \left(X_{q_x}^{\ell' \ell} b_{q_x, \ell' \ell} + Z_{q_x}^{\ell' \ell} b_{-q_x, \ell' \ell}^\dagger \right), \quad (\text{A11})$$

which satisfies $[p_{q_x}, H] = \omega_{q_x}^{\text{pol}} p_{q_x}$, one has to diagonalize the corresponding Bogoliubov matrix \mathcal{M}_{q_x} . The polaritonic frequencies $\omega_{q_x}^{\text{pol}}$ are the positive eigenvalues of \mathcal{M}_{q_x} , given by the solutions of the equation $\det(\mathcal{M}_{q_x} - \omega) = 0$. The determinant can be written as

$$\det(\mathcal{M}_{q_x} - \omega) = \left[1 + [1 - \mathcal{I}_{q_x}(\omega)] \sum_{n_z \text{ odd}} \frac{4D_{q_x}^{1,1} \omega_{q_x, 1}^{\text{cav}}}{(\omega_{q_x, n_z}^{\text{cav}})^2 - \omega^2} \right] \times \prod_{\text{odd } n_z} [\omega^2 - (\omega_{q_x, n_z}^{\text{cav}})^2] \prod_{\ell \leq \nu < \ell'} [\omega^2 - (\omega_{\ell' \ell}^{\text{LL}})^2], \quad (\text{A12})$$

where we defined $\mathcal{I}_{q_x}(\omega)$ as

$$\mathcal{I}_{q_x}(\omega) = \frac{1}{\nu m^* l_B^2} \sum_{\ell \leq \nu < \ell'} \frac{\omega_{\ell' \ell}^{\text{LL}} [g_{q_x}^{\ell' \ell}]^2}{(\omega_{\ell' \ell}^{\text{LL}})^2 - \omega^2}. \quad (\text{A13})$$

Using the fact that

$$\sum_{n_z \text{ odd}} \frac{1}{n_z^2 + u^2} = \frac{\pi}{4u} \tanh \frac{\pi u}{2}, \quad (\text{A14})$$

we can evaluate the n_z sum in Eq. (A12) explicitly:

$$\sum_{n_z \text{ odd}} \frac{4}{(\omega_{q_x, n_z}^{\text{cav}})^2 - \omega^2} = \frac{\epsilon L_z / c^2}{\sqrt{q_x^2 - \epsilon \omega^2 / c^2}} \tanh \frac{L_z \sqrt{q_x^2 - \epsilon \omega^2 / c^2}}{2}. \quad (\text{A15})$$

Equating to zero the first prefactor in Eq. (A12), we obtain the equation for the polariton frequencies, the main analytical result of the present paper:

$$\coth \frac{L_z \sqrt{q_x^2 - \epsilon \omega^2 / c^2}}{2} = \frac{e^2}{c} \frac{2\pi n_{\text{qw}} n_e}{m^*} \frac{\mathcal{I}_{q_x}(\omega) - 1}{\sqrt{c^2 q_x^2 - \epsilon \omega^2}}, \quad (\text{A16})$$

which is equivalent to Eqs. (5) and (6) of the main text.

In the numerical calculations, we diagonalized the Bogoliubov matrix in a truncated basis of LLs and cavity modes, and checked for convergence. Typically, this required 50 LLs and n_z up to 10^4 for a given q_x .

Appendix B: Effective action approach

Let us describe the system by its Euclidean action S (weight e^{-S}) in the imaginary time τ varying in the interval

$0 \leq \tau \leq \beta$, where $\beta = 1/T$ is the inverse temperature that we will eventually send to infinity ($T \rightarrow 0$). The action consists of two parts, $S = S_{\text{cav}} + S_{2\text{DEG}}$. The action of the free cavity field is

$$S_{\text{cav}}[\mathbf{A}^{\text{cav}}] = \int_0^\beta d\tau \int d^3\mathbf{r} \left[\frac{\varepsilon(\partial_\tau \mathbf{A}^{\text{cav}})^2}{8\pi c^2} + \frac{|\nabla \times \mathbf{A}^{\text{cav}}|^2}{8\pi} \right]. \quad (\text{B1})$$

Here \mathbf{A}^{cav} is the vector potential of the cavity field in the Coulomb gauge, $\nabla \cdot \mathbf{A}^{\text{cav}} = 0$, while ε is the dielectric constant of the material filling the cavity. The electrons of the 2DEG, whose number is assumed to be fixed, are described by the action

$$S_{2\text{DEG}}[\psi^*, \psi, \mathbf{A}] = \int_0^\beta d\tau \int dx dy \psi^\dagger \left(\frac{\partial}{\partial \tau} + \mathcal{H}_{2\text{DEG}}^{\otimes n_{\text{qw}}} \right) \psi, \quad (\text{B2})$$

where $\psi(x, y)$, $\psi^\dagger(x, y)$ are $2n_{\text{qw}}$ -component vectors of Grassmann variables, corresponding to two electron spin projections in each of the n_{qw} quantum wells. The single-electron Hamiltonian $\mathcal{H}_{2\text{DEG}}$ is given by Eq. (1) with $\mathbf{A} = \mathbf{A}^{\text{ext}} + \mathbf{A}^{\text{cav}}$. $\mathcal{H}_{2\text{DEG}}$ a 2×2 matrix in the spin space, and in Eq. (B2) it should be replicated n_{qw} times which is indicated by the superscript $\otimes n_{\text{qw}}$.

Let us integrate out the electrons and obtain the effective action $S_{\text{eff}}[\mathbf{A}^{\text{cav}}]$ for the field only. It is convenient to pass to Matsubara frequencies

$$\mathbf{A}^{\text{cav}}(\mathbf{r}, \tau) = T \sum_n \mathbf{A}^{\text{cav}}(\mathbf{r}, \omega_n) e^{-i\omega_n \tau}, \quad (\text{B3})$$

where $\omega_n = 2\pi nT$, and $\mathbf{A}^{\text{cav}}(-\omega_n) = [\mathbf{A}^{\text{cav}}(\omega_n)]^*$. Then the effective action can be written as a series in powers of \mathbf{A}^{cav} :

$$\begin{aligned} S_{\text{eff}} &= \frac{T}{2} \sum_{\omega_n} \int d^3\mathbf{r} \left(\frac{\varepsilon \omega_n^2}{4\pi c^2} |\mathbf{A}^{\text{cav}}|^2 + \frac{1}{4\pi} |\nabla \times \mathbf{A}^{\text{cav}}|^2 \right) \\ &\quad - \frac{1}{c} \int d^3\mathbf{r} \mathbf{j}^{\text{eq}}(\mathbf{r}) \cdot \mathbf{A}^{\text{cav}}(\mathbf{r}, \omega_n = 0) \\ &\quad + \frac{T}{2c^2} \sum_{\omega_n} \int d^3\mathbf{r} d^3\mathbf{r}' \mathcal{Q}_{ij}(\mathbf{r}, \mathbf{r}', i\omega_n) \\ &\quad \quad \times A_i^{\text{cav}}(\mathbf{r}, -\omega_n) A_j^{\text{cav}}(\mathbf{r}', \omega_n) \\ &\quad + \frac{T^2}{6c^3} \sum_{\omega_n, \omega_{n'}} \int d^3\mathbf{r} d^3\mathbf{r}' d^3\mathbf{r}'' \mathcal{Q}_{ijk}^{(2)}(\mathbf{r}, \mathbf{r}', \mathbf{r}''; i\omega_n, i\omega_{n'}) \\ &\quad \quad \times A_i^{\text{cav}}(\mathbf{r}, -\omega_n - \omega_{n'}) A_j^{\text{cav}}(\mathbf{r}', \omega_n) A_k(\mathbf{r}'', \omega_{n'}) \\ &\quad + \dots, \end{aligned} \quad (\text{B4})$$

where the kernels $\mathcal{Q}^{(n)}$ are given by the sum of electronic loops where the vertices $\psi^* \psi \mathbf{A}^{\text{cav}}$ and $\psi^* \psi (\mathbf{A}^{\text{cav}})^2$ appear n_1 and n_2 times, respectively, and $n_1 + 2n_2 = n + 1$. Generally speaking, the system is allowed to have an equilibrium current density, $\mathbf{j}^{\text{eq}}(\mathbf{r})$, since it is placed in an external magnetic field and time reversal invariance is broken; in our specific case $\mathbf{j}^{\text{eq}} = 0$.

Analytical continuation in frequency of the kernels $\mathcal{Q}^{(n)}$ from the positive imaginary semiaxis $\omega = i\omega_n$, $\omega_n > 0$, to the real axis ω , gives the response functions which determine the response of the current density $\delta \mathbf{j}$ to a change in the vector potential, $\mathbf{A} = \mathbf{A}^{\text{ext}} + \delta \mathbf{A}$; in the linear order,

$$\delta j_k(\mathbf{r}, \omega) = - \int d^3\mathbf{r}' \mathcal{Q}_{kl}(\mathbf{r}, \mathbf{r}', \omega) \frac{\delta A_l(\mathbf{r}', \omega)}{c}. \quad (\text{B5})$$

The polariton modes of the coupled system are determined by the quadratic part of S_{eff} whose kernel is

$$\begin{aligned} \mathcal{D}^{-1}(\mathbf{r}, \mathbf{r}', i\omega_n) &= \frac{\delta(\mathbf{r} - \mathbf{r}')}{4\pi} \left[\varepsilon(\mathbf{r}) \frac{\omega_n^2}{c^2} + \nabla \times \nabla \times \right] \\ &\quad + \frac{1}{c^2} \mathcal{Q}_{ij}(\mathbf{r}, \mathbf{r}', i\omega_n). \end{aligned} \quad (\text{B6})$$

Namely, the polariton frequencies are solutions of the equation $\det \mathcal{D}^{-1}(\omega) = 0$, where $\mathcal{D}^{-1}(\omega)$ is the analytical continuation of $\mathcal{D}^{-1}(i\omega_n)$ from the positive imaginary semiaxis and the determinant should be understood in the operator sense. Equivalently, the polariton eigenmodes are the nonzero solutions of

$$\left[\varepsilon \frac{\omega^2}{c^2} + \nabla^2 \right] A_i(\mathbf{r}) = \frac{4\pi}{c^2} \int \mathcal{Q}_{ij}(\mathbf{r}, \mathbf{r}', \omega) A_j(\mathbf{r}') d^3\mathbf{r}', \quad (\text{B7})$$

with $\nabla \cdot \mathbf{A} = 0$, which is just the third Maxwell's equation with a source current. The SQPT corresponds to the appearance of an unstable direction in the quadratic form with the kernel $\mathcal{D}^{-1}(\omega = 0)$.

It should be noted that the zero-frequency limit of the Kubo susceptibility $\mathcal{Q}(\omega)$, which was obtained by the analytical continuation of the Matsubara susceptibility $\mathcal{Q}(i\omega_n)$ from the positive imaginary semiaxis $\omega_n > 0$, is, generally speaking, different from the value of the Matsubara susceptibility $\mathcal{Q}(i\omega_n)$ taken directly at $\omega_n = 0$. The Kubo limit $\mathcal{Q}(\omega \rightarrow 0)$ corresponds to evaluating the current with LL wave functions perturbed by a static $\delta \mathbf{A}$ and keeping the LL populations unperturbed; the Matsubara limit $\mathcal{Q}(i\omega_n = 0)$ also takes into account the change in the LL populations which occurs because of the shift of the LL energies while the temperature and the chemical potential are kept fixed. In other words, they correspond to different order of limits $\omega \rightarrow 0$ and population relaxation time to infinity. In our case, we are working at zero temperature and fixed electron density, rather than at fixed chemical potential. Thus, we take the Kubo limit.

By gauge invariance, a static vector potential $\mathbf{A}(\mathbf{r})$ can affect observable quantities only via the associated magnetic field $\mathbf{B} = \nabla \times \mathbf{A}$. Also, at zero frequency the continuity equation for the current density requires $\nabla \cdot \mathbf{j} = 0$, so one can write $\mathbf{j} = c \nabla \times \mathbf{M}$, where \mathbf{M} is called magnetization. Then it is convenient to express the response function $\mathcal{Q}_{ij}(\mathbf{r}, \mathbf{r}', \omega = 0)$ in terms of the static magnetic susceptibility $\chi_{ij}(\mathbf{r}, \mathbf{r}')$, which determines the response of the magnetization $\delta \mathbf{M}$ to a magnetic field perturbation $\delta \mathbf{B}$ on top of \mathbf{B}^{ext} . Then,

$$\frac{1}{c^2} \mathcal{Q}_{ij}(\mathbf{r}, \mathbf{r}', \omega = 0) = -e_{ikl} e_{jmn} \frac{\partial^2 \chi_{ln}(\mathbf{r}, \mathbf{r}')}{\partial x_k \partial x'_m}, \quad (\text{B8})$$

where e_{ikl} is the Levi-Civita antisymmetric tensor.

Now we proceed to evaluation of the response function $Q_{kl}(\mathbf{r}, \mathbf{r}', \omega)$ for the 2DEG with the Rashba spin-orbit coupling under an external magnetic field. The single-electron 2D current density operator, corresponding to Hamiltonian (1) for a single quantum well is given by

$$\mathbf{j} = -\frac{\partial \mathcal{H}_{2\text{DEG}}}{\partial(\mathbf{A}/c)} = -\frac{e}{m^*} \mathbf{p} - e\alpha[\mathbf{u}_z \times \boldsymbol{\sigma}] - \frac{e^2}{m^*} \frac{\mathbf{A}}{c}, \quad (\text{B9})$$

where $\mathbf{u}_{x,y,z}$, denotes the unit vectors in the respective directions. As $\mathbf{A} = \mathbf{A}^{\text{ext}} + \delta\mathbf{A}$, the term proportional to $\delta\mathbf{A}$ gives the diamagnetic contribution to the response, while the rest should be plugged in the Kubo formula. We neglect the 2DEG thickness compared to all other length scales, so all quantum wells contribute additively and the response has the form

$$Q_{kl}(\mathbf{r}, \mathbf{r}', \omega) = \int \frac{d^2\mathbf{q}}{(2\pi)^2} e^{iq_x(x-x') + iq_y(y-y')} Q_{kl}(\mathbf{q}, \omega) \times \delta(z - L_z/2) \delta(z' - L_z/2). \quad (\text{B10})$$

We are interested in the Q_{yy} component at $\mathbf{q} = q_x \mathbf{u}_x$:

$$Q_{yy}(q_x, \omega) = \frac{2n_{\text{qw}}}{L_x L_y} \sum_{\ell \leq \nu < \ell'} \sum_{p_x, p'_x} \frac{\omega_{\ell'\ell}^{\text{LL}} |\langle \ell, p_x | j_y(q_x) | \ell', p'_x \rangle|^2}{\omega^2 - (\omega_{\ell'\ell}^{\text{LL}})^2} + \frac{n_{\text{qw}} n_e e^2}{m^*}, \quad (\text{B11})$$

where the first term comes from the Kubo formula and the last is the diamagnetic one.

Evaluation of the current matrix elements between the LL eigenstates (A1) gives

$$\begin{aligned} \langle \ell, p_x | j_y(q_x) | \ell', p'_x \rangle &\equiv e \int dx dy e^{-iq_x x} \\ &\times \left[\frac{i}{2m^*} \left(\psi_{\ell, p_x}^\dagger \frac{d\psi_{\ell', p'_x}}{dy} - \frac{d\psi_{\ell, p_x}^\dagger}{dy} \psi_{\ell', p'_x} \right) - \alpha \psi_{\ell, p_x}^\dagger \sigma_x \psi_{\ell', p'_x} \right] \\ &= -i \frac{e}{\sqrt{2} m^* l_B} g_{q_x}^{\ell'\ell} \delta_{p'_x, p_x + q_x}, \end{aligned} \quad (\text{B12})$$

where $g_{q_x}^{\ell'\ell}$ is given by Eq. (7). As a result,

$$Q_{yy}(q_x, \omega) = \frac{n_{\text{qw}} n_e e^2}{m^*} [-\mathcal{I}_{q_x}(\omega) + 1], \quad (\text{B13})$$

where $\mathcal{I}_{q_x}(\omega)$ is given by Eq. (A13).

Equation (B7) becomes

$$\begin{aligned} &\left(\varepsilon \frac{\omega^2}{c^2} - q_x^2 + \frac{d^2}{dz^2} \right) A_y(z) \\ &= \frac{4\pi}{c^2} \delta(z - L_z/2) Q_{yy}(q_x, \omega) A_y(L_z/2), \end{aligned} \quad (\text{B14})$$

with the boundary conditions $A_y(0) = A_y(L_z) = 0$. It has one family of solutions, $A_y(z) \propto \sin(\pi n_z z/L_z)$ with even n_z , corresponding to the cavity modes which remain decoupled from the 2DEG since $A_y(L_z/2) = 0$. The other family

can be represented as

$$A_y(z) \propto \sinh(\kappa ||z - L_z/2| - L_z/2|), \quad \kappa \equiv \sqrt{q_x^2 - \varepsilon \frac{\omega^2}{c^2}}. \quad (\text{B15})$$

It has a jump of the derivative at $z = L_z/2$, which should be matched to the right-hand side of Eq. (B14), yielding

$$-2\kappa \cosh \frac{\kappa L_z}{2} = \frac{4\pi}{c^2} Q_{yy}(q_x, \omega) \sinh \frac{\kappa L_z}{2}, \quad (\text{B16})$$

which is equivalent to Eq. (5) of the main text and Eq. (A16).

Appendix C: Estimate for the ‘‘superradiant’’ phase width

Let us choose some LL crossing, $\varepsilon_{\eta_1,+} = \varepsilon_{\eta_2,-}$, and focus on α close to that given by Eq. (3) which is denoted by α_c . The LL indices η_1, η_2 satisfy $\eta_1 + \eta_2 = \nu$, and we denote $\eta_1 - \eta_2 = \delta$. We will assume $\nu \gg 1$, and the order-of-magnitude estimate is expected to be valid for $\nu \sim 1$ as well. The dimensionless Rashba coupling strength corresponding to the crossing is then

$$\gamma_c \equiv \alpha_c m^* l_B \approx \sqrt{\frac{\delta^2 - 1}{4\nu}} \ll 1. \quad (\text{C1})$$

When α is detuned away from the crossing, keeping both the magnetic field and the filling constant, the LL energy difference becomes

$$\omega^{\text{LL}} = |\varepsilon_{\eta_1,+} - \varepsilon_{\eta_2,-}| \approx \sqrt{4\nu \frac{\delta^2 - 1}{\delta^2}} \frac{|\alpha - \alpha_c|}{l_B}. \quad (\text{C2})$$

To estimate the coupling strength g_{q_x} at the crossing, we use the well-known asymptotic expression for the generalized Laguerre polynomials with large index in terms of the Bessel function of the first kind, J , which gives

$$\Theta_{n_2}^{n_1} \approx J_{|n_1 - n_2|} \left(\sqrt{2(n_1 + n_2)\xi} \right). \quad (\text{C3})$$

Next, we need to find the angles $\theta_{\eta_1,+}$ and $\theta_{\eta_2,-}$. To the leading order in $1/\sqrt{\nu}$,

$$\tan \theta_{\eta_1,+} = -\cot \theta_{\eta_2,-} = \sqrt{\frac{|\delta| - 1}{|\delta| + 1}}, \quad (\text{C4})$$

and thus $\theta_{\eta_2,-} = \theta_{\eta_1,+} + \pi/2 + O(1/\nu)$. As a result, the leading terms in the coupling g_{q_x} cancel. This happens because of approximate orthogonality of the spin part of the wave functions for $|\eta_1 - \eta_2| \ll \eta_1, \eta_2$ and $s_1 = -s_2$.

Expansion to the next order will generate many terms; the resulting bulky expressions are not very informative. To obtain an order-of-magnitude estimate, it is sufficient to notice that the coupling strength can be written in the form

$$|g_{q_x}^{+-}|^2 = \frac{1}{\nu} \mathcal{G}_\delta(\sqrt{\nu} q_x l_B), \quad (\text{C5})$$

where for $\delta \sim 1$ the function $\mathcal{G}_\delta(x)$ decays faster than x at $x \rightarrow 0$, reaches the first maximum at $x \sim 1$, and the width of

this maximum is also ~ 1 . Then, assuming that $Q_{yy}(q_x, \omega = 0)$ is dominated by a single term corresponding to the LL crossing under consideration and setting $\coth(q_x L_z/2) \rightarrow 1$, we can write Eq. (5) of the main text as

$$\Lambda \sqrt{\nu} q_x l_B = \mathcal{G}_\delta(\sqrt{\nu} q_x l_B), \quad \Lambda \sim |\alpha - \alpha_c| \frac{(m^* c)^2 \nu^2}{n_{\text{qw}} n_e e^2}. \quad (\text{C6})$$

This equation has no solutions for q_x if $\Lambda \gg 1$; solutions appear when $\Lambda \sim 1$ [Eq. (9) of the main text]; then the typical scale of q_x and the width of the unstable q_x interval are determined by $\sqrt{\nu} q_x l_B \sim 1$.

-
- [1] R. H. Dicke, *Phys. Rev.* **93**, 99 (1954).
[2] C. Ciuti, G. Bastard, and I. Carusotto, *Phys. Rev. B* **72**, 115303 (2005).
[3] P. Forn-Díaz, L. Lamata, E. Rico, J. Kono, and E. Solano, *Rev. Mod. Phys.* **91**, 025005 (2019).
[4] K. Hepp and E. H. Lieb, *Annals of Physics* **76**, 360 (1973).
[5] C. Emary and T. Brandes, *Phys. Rev. E* **67**, 066203 (2003).
[6] G. Scalari, C. Maissen, D. Turčinková, D. Hagenmüller, S. De Liberato, C. Ciuti, C. Reichl, D. Schuh, W. Wegscheider, M. Beck, and J. Faist, *Science* **335**, 1323 (2012), <http://science.sciencemag.org/content/335/6074/1323.full.pdf>.
[7] J. Keller, G. Scalari, F. Appugliese, C. Maissen, J. Haase, M. Failla, M. Myronov, D. R. Leadley, J. Lloyd-Hughes, P. Nataf, and J. Faist, *ArXiv e-prints* (2018), [arXiv:1708.07773](https://arxiv.org/abs/1708.07773).
[8] K. Rzażewski, K. Wódkiewicz, and W. Żakowicz, *Phys. Rev. Lett.* **35**, 432 (1975).
[9] P. Nataf and C. Ciuti, *Nature Communications* **1**, 72 (2010).
[10] Y. Todorov and C. Sirtori, *Phys. Rev. B* **85**, 045304 (2012).
[11] M. Hayn, C. Emary, and T. Brandes, *Phys. Rev. A* **86**, 063822 (2012).
[12] L. Chiroli, M. Polini, V. Giovannetti, and A. H. MacDonald, *Phys. Rev. Lett.* **109**, 267404 (2012).
[13] M. Bamba and T. Ogawa, *Phys. Rev. A* **90**, 063825 (2014).
[14] E. Rousseau and D. Felbacq, *Scientific Reports* **7**, 11115 (2017).
[15] G. M. Andolina, F. M. D. Pellegrino, V. Giovannetti, A. H. MacDonald, and M. Polini, *arXiv e-prints*, [arXiv:1905.11227](https://arxiv.org/abs/1905.11227) (2019), [arXiv:1905.11227 \[cond-mat.mes-hall\]](https://arxiv.org/abs/1905.11227).
[16] F. Dimer, B. Estienne, A. S. Parkins, and H. J. Carmichael, *Phys. Rev. A* **75**, 013804 (2007).
[17] F. m. c. Damanet, A. J. Daley, and J. Keeling, *Phys. Rev. A* **99**, 033845 (2019).
[18] K. Baumann, C. Guerlin, F. Brennecke, and T. Esslinger, *Nature* **464**, 1301 (2010).
[19] J. M. Knight, Y. Aharonov, and G. T. C. Hsieh, *Phys. Rev. A* **17**, 1454 (1978).
[20] P. Nataf and C. Ciuti, *Phys. Rev. Lett.* **104**, 023601 (2010).
[21] P. Nataf and C. Ciuti, *Phys. Rev. Lett.* **107**, 190402 (2011).
[22] M. Devoret, S. Girvin, and R. Schoelkopf, *Annalen der Physik* **16**, 767 (2007).
[23] J. Keeling, *Journal of Physics: Condensed Matter* **19**, 295213 (2007).
[24] A. Vukics, T. Grießer, and P. Domokos, *Phys. Rev. A* **92**, 043835 (2015).
[25] F. M. D. Pellegrino, V. Giovannetti, A. H. MacDonald, and M. Polini, *Nature Communications* **7**, 13355 (2016).
[26] G. Mazza and A. Georges, *Phys. Rev. Lett.* **122**, 017401 (2019), the mistake of this paper is to conclude that the excitonic instability is accompanied by spontaneous generation of a static and spatially uniform average value of the vector potential.
[27] D. Shoenberg, *Magnetic Oscillations in Metals* (Cambridge University Press, 1984).
[28] C. Weisbuch, M. Nishioka, A. Ishikawa, and Y. Arakawa, *Phys. Rev. Lett.* **69**, 3314 (1992).
[29] Y. A. Bychkov and É. I. Rashba, *JETP Letters* **39**, 78 (1984).
[30] S. Becker, M. Liebmann, T. Mashoff, M. Pratzter, and M. Morgenstern, *Phys. Rev. B* **81**, 155308 (2010).
[31] D. Hernangómez-Pérez, J. Ulrich, S. Florens, and T. Champel, *Phys. Rev. B* **88**, 245433 (2013).
[32] K. Kakazu and Y. S. Kim, *Phys. Rev. A* **50**, 1830 (1994).
[33] D. Hagenmüller, S. De Liberato, and C. Ciuti, *Phys. Rev. B* **81**, 235303 (2010).
[34] P. Nataf, A. Baksic, and C. Ciuti, *Phys. Rev. A* **86**, 013832 (2012).
[35] A. Baksic and C. Ciuti, *Phys. Rev. Lett.* **112**, 173601 (2014).
[36] T. Champel and S. Florens, *Phys. Rev. B* **80**, 161311 (2009).
[37] J. M. Luttinger, *Phys. Rev.* **102**, 1030 (1956).
[38] R. Winkler, M. Merkler, T. Darnhofer, and U. Rössler, *Phys. Rev. B* **53**, 10858 (1996).
[39] R. Winkler, *Phys. Rev. B* **62**, 4245 (2000).
[40] R. Moriya, K. Sawano, Y. Hoshi, S. Masubuchi, Y. Shiraki, A. Wild, C. Neumann, G. Abstreiter, D. Bougeard, T. Koga, and T. Machida, *Phys. Rev. Lett.* **113**, 086601 (2014).
[41] C. Maissen, G. Scalari, F. Valmorra, M. Beck, J. Faist, S. Cibella, R. Leoni, C. Reichl, C. Charpentier, and W. Wegscheider, *Phys. Rev. B* **90**, 205309 (2014).